



Late Pleistocene Human Skull from Hofmeyr, South Africa, and Modern Human Origins

F. E. Grine, *et al.*

Science **315**, 226 (2007);

DOI: 10.1126/science.1136294

The following resources related to this article are available online at www.sciencemag.org (this information is current as of January 12, 2007):

Updated information and services, including high-resolution figures, can be found in the online version of this article at:

<http://www.sciencemag.org/cgi/content/full/315/5809/226>

Supporting Online Material can be found at:

<http://www.sciencemag.org/cgi/content/full/315/5809/226/DC1>

This article **cites 11 articles**, 4 of which can be accessed for free:

<http://www.sciencemag.org/cgi/content/full/315/5809/226#otherarticles>

This article appears in the following **subject collections**:

Anthropology

<http://www.sciencemag.org/cgi/collection/anthro>

Information about obtaining **reprints** of this article or about obtaining **permission to reproduce this article** in whole or in part can be found at:

<http://www.sciencemag.org/help/about/permissions.dtl>

23. A. A. Sinityn, N. D. Praslov, Yu. S. Svezhentsev, L. D. Sulerzhitskii, in *Radiouglerodnaya khronologiya paleolita Vostochnoi Evropy i Severnoi Azii. Problemy i perspektivy*, A. A. Sinityn, N. D. Praslov, Eds. (Russian Academy of Sciences, St. Petersburg, 1997), pp. 21–66.
24. R. G. Fairbanks *et al.*, *Quat. Sci. Rev.* **24**, 1781 (2005).
25. CalPal Online (www.calpal-online.de).
26. J. F. Hoffecker, *Desolate Landscapes: Ice-Age Settlement in Eastern Europe* (Rutgers Univ. Press, New Brunswick, NJ, 2002).
27. G. M. Levkovskaya, in *Paleoekologiya drevnego cheloveka*, I. K. Ivanova, N. D. Praslov, Eds. (Nauka, Moscow, 1977), pp. 74–83.
28. E. A. Spiridonova, *Evolutsiya rastitel'nogo pokrova basseina Dona v verkhnem pleistotsene-golotsene* (Nauka, Moscow, 1991).
29. N. J. Shackleton, R. G. Fairbanks, T.-C. Chiu, F. Parrenin, *Quat. Sci. Rev.* **23**, 1513 (2004).
30. N. K. Vereshchagin, I. E. Kuz'mina, in *Paleolit Kostenkovsko-Borshchevskogo raiona na Donu 1879–1979*, N. D. Praslov, A. N. Rogachev, Eds. (Nauka, Leningrad, 1982), pp. 223–232.
31. We thank D. M. Pyle and B. J. Carter for analyses of volcanic ash samples, J. Pierson and J. Gomez for assistance with OSL dating, Ya. I. Starobogatova for the identification of fossil shells from Kostenki 14, and S. L. Kuhn for review of an earlier draft. Figure 1 was

prepared by the University of Wisconsin Cartography Lab. Supported by NSF grants BCS-0132553 and BCS-0442164, Leakey Foundation 2001 and 2004 general grants, and Russian Foundation for Basic Research grant N05-06-80329a. The Leakey Foundation grants were administered by the Illinois State Museum.

Supporting Online Material

www.sciencemag.org/cgi/content/full/315/5809/223/DC1
Tables S1 to S5

References

2 August 2006; accepted 13 November 2006
10.1126/science.1133376

Late Pleistocene Human Skull from Hofmeyr, South Africa, and Modern Human Origins

F. E. Grine,^{1*} R. M. Bailey,² K. Harvati,³ R. P. Nathan,⁴ A. G. Morris,⁵ G. M. Henderson,⁶ I. Ribot,⁷ A. W. G. Pike⁸

The lack of Late Pleistocene human fossils from sub-Saharan Africa has limited paleontological testing of competing models of recent human evolution. We have dated a skull from Hofmeyr, South Africa, to 36.2 ± 3.3 thousand years ago through a combination of optically stimulated luminescence and uranium-series dating methods. The skull is morphologically modern overall but displays some archaic features. Its strongest morphometric affinities are with Upper Paleolithic (UP) Eurasians rather than recent, geographically proximate people. The Hofmeyr cranium is consistent with the hypothesis that UP Eurasians descended from a population that emigrated from sub-Saharan Africa in the Late Pleistocene.

Most genetic studies indicate that all contemporary humans owe their ancestry to a sub-Saharan African population, extant between 100 and 200 thousand years ago (ka) (1–3). A number of genetic studies further suggest that modern humans left sub-Saharan Africa in the Late Pleistocene, between 65 and 25 ka (1–6). The middle of this range (~45 to 35 ka) corresponds not only with the appearance of Later Stone Age (LSA) industries in sub-Saharan Africa (7) but also with the earliest Upper Paleolithic (UP) industries and human skeletons in Eurasia (8). However, other genetic data appear to suggest substantial non-African contributions to the genomes of modern human populations, and

these data have been interpreted as being inconsistent with any population bottleneck associated with a recent African exodus (9, 10).

The human palaeontological record might be used to test predictions from these hypotheses. Craniometric data tend to differentiate recent human populations in accord with their geographic distributions and genetic relationships (11–15). Eurasian UP crania do not particularly resemble those of earlier Eurasian Neandertals (16), nor are they especially similar to recent human crania from sub-Saharan Africa (12). Thus, we should not expect to see any special similarity between the UP Eurasians and contemporaneous sub-Saharan Africans in the absence of a Late Pleistocene exodus from sub-Saharan Africa.

Although there are several variably complete crania from North Africa that date to between about 40 and 20 ka (from Dar es Soltan, Morocco; and Nazlet Khater and Wadi Kubbania, Egypt), the only sub-Saharan specimen in LSA context that has been claimed to pre-date 20 ka is an infant mandible from Origstad Shelter, South Africa, and it may be substantially younger (17). The lack of Late Pleistocene human remains from sub-Saharan Africa has resulted in an inability to test competing models of human evolution (18).

We report on a nearly complete human cranium from Hofmeyr, South Africa, and its dating to 36.2 ± 3.3 ka. The skull was discovered in 1952 in a dry channel bed of the Vlekpoot River ($25^{\circ}58'E$, $31^{\circ}34'S$) near the town of

Hofmeyr, Eastern Cape Province, South Africa. The endocranial cavity, orbits, nasal cavity, and palate were filled with an indurated carbonate-sand matrix. No other bones or archaeological artefacts were reportedly found in the vicinity at the time of the skull's discovery, and within a decade, the channel had become filled by silt, after the construction of an anti-erosion weir downstream. This precludes any possibility of locating the original position of the specimen or of directly dating the surrounding sediments.

In the 1960s, a substantial portion of the left parietal bone was removed, presumably in an attempt to obtain a radiocarbon date, although no date has ever been published. Another, smaller bone sample was submitted by us to the University of Oxford Radiocarbon Accelerator Unit to assess its amenability to accelerator mass spectrometry (AMS) ^{14}C dating, but it lacked sufficient collagen for an accurate age determination (19). Instead, we estimated the burial age of the skull by dating the residence time of the matrix filling the endocranial cavity, using a combination of optically stimulated luminescence and uranium-series dating methods, coupled through a radiation-field model. The length of time between death and incorporation of the sediment within the skull is expected to be short, because the loss of organic material after death would be rapid (days to months). Furthermore, the skull's relatively good state of preservation suggests that it had neither been uncovered long before nor transported any substantial distance before its discovery (the force required to scour the innermost sediments would certainly have resulted in substantial damage). Additional evidence for a single infilling episode comes from the consistency of the dates determined from the samples of endocranial matrix.

The signals measured in luminescence dating are a consequence of the absorption by mineral grains of ionizing radiation from low concentrations of radionuclides that are naturally present in the sediment and from cosmic rays (20). Luminescence dating methods provide estimates of the total ionizing radiation dose [D_e , in units of grays (Gy)] absorbed by sediment (in this case quartz) grains since their burial. Estimation of burial age is possible if the radiation dose rate (D' , in units of Gy/ka) is known. In the simplest case, where D' is constant in time, $\text{age} = D_e/D'$. Three samples of endocranial sediment were extracted

¹Departments of Anthropology and Anatomical Sciences, Stony Brook University, Stony Brook, NY 11794-4364, USA.

²School of Geography and the Environment, University of Oxford, South Parks Road, Oxford, OX1 3QY, UK. ³Max Planck Institute for Evolutionary Anthropology, Deutscher Platz 6, 04103 Leipzig, Germany. ⁴Research Laboratory for Archaeology and the History of Art, University of Oxford, South Parks Road, Oxford, OX1 3QY, UK. ⁵Department of Human Biology, University of Cape Town, Observatory 7925, Cape Town, South Africa. ⁶Department of Earth Sciences, University of Oxford, South Parks Road, Oxford, OX1 3PR, UK. ⁷Département d'Anthropologie, Université de Montréal, CP 6128, Succursale Centre-Ville, Montréal, Québec H3C 3J7, Canada. ⁸Department of Archaeology and Anthropology, University of Bristol, 43 Woodland Road, Bristol, BS8 1UU, UK.

*To whom correspondence should be addressed. E-mail: fgrine@notes.cc.sunysb.edu

under red-light conditions from the central portion of the endocranial cavity, and successful measurements of D_e were made on aliquots of refined quartz from each sample. Estimation of D' for the sampled grains is more complex than is typically the case in luminescence dating, due mainly to the presence of carbonate in the sediment and to a measured disequilibrium in the U decay series. Carbonate has the potential to reduce D' by radiation attenuation or to increase it by the incorporation of mobile U. A further complication is that bone adsorbs mobile U; thus, the skull itself may contribute an additional local γ -dose component to D' . These factors combine to give both a time and space dependence to D' . The date of carbonate formation was assessed as 24.0 ± 5.2 ka with the use of a Th/U isochron (21), and the deposition of energy within the interior of the skull (giving D') during burial was modeled with a three-dimensional (3D) Monte Carlo radiation transport model (22, 23) (with the model geometry defined with data from a computed tomography scan of the skull). From this modeling, the time required for the total radiation dose (defined by the luminescence measurements) to have been absorbed by the quartz grains could be estimated, yielding ages for the three samples of 40.9 ± 4.2 , 33.0 ± 2.5 , and 34.7 ± 3.4 ka. These combine as 36.2 ± 3.3 ka (1σ) for the depositional age of the endocranial sediment (24).

The skull has suffered post-recovery mishandling, with the resultant loss of the anterior part of the lower facial skeleton, the angle of the mandible, the mastoid process of the right temporal, and much of the occipital. However, it was photographed and measured before this damage (Fig. 1), and there is no distortion of the remaining parts of the cranium. We incorporated the missing parts from these photographs and used measurements recorded before the damage.

The Hofmeyr skull is fully adult; the coronal suture is obliterated and the third molars are heavily worn. It suffered antemortem trauma to the lateral margin of the right orbit, which exhibits a healed or partially healed depressed fracture. This crushing, together with associated bony exostoses along its posterior margin, exaggerate the thickness of the frontal process of the zygomatic. The anterior surface of the right supra-orbital torus appears to have been cut away.

Hofmeyr presents an overall picture of morphological modernity in its steeply rising frontal and high rounded vault, the maximum breadth of which is situated high on the parietals. Weak frontal eminences recede laterally from a broad low midline keel that rises vertically from the glabella. The skull is large and robust. The maximum estimated length and breadth of the neurocranium, as well as most measurements of the facial skeleton, lie at or exceed two standard deviations (SD) of the means for modern African males, whereas they lie within these limits for Late Pleistocene crania from Eurasia and North Africa (table S3). Narrow nasal bones are bounded by very broad (~15.0 mm), relatively flat frontal

processes of the maxillae. The pyriform aperture is broad in comparison to that of most Eurasian UP crania. The infraorbital plate is tall and flat and lacks an inframalar curve. As such, it differs from the condition that characterizes recent southern African crania (12, 25). Frontal and parietal thickness (6 to 7 mm) is comparable to that of recent humans.

The glabella projects to a greater degree than in modern Africans but is comparable to that of UP crania. The supraorbital tori of Hofmeyr are moderately well developed and continuous, lacking the separation of the medial supraorbital eminence and lateral superciliary arch that is characteristic of recent humans. Although the supraorbital torus is comparable in thickness to that in UP crania, its continuous nature represents a more archaic morphology (26). In this regard, Hofmeyr is more primitive than later sub-Saharan LSA and North African UP specimens (such as

Lukenya Hill and Wadi Kubaniya), even though they may have a somewhat thicker medial supra-orbital eminence. Despite its glabellar prominence and capacious maxillary sinuses, Hofmeyr exhibits only incipient frontal sinus development, a condition that is uncommon among European UP crania (27).

The mandibular ramus has a well-developed gonial angle, and the slender coronoid process is equivalent in height to the condyle. The mandibular (sigmoid) notch is deep and symmetrical, and its crest intersects the lateral third of the condyle. The anterior margin of the ramus is damaged, but it is clear that there was no retro-molar gap.

The Hofmeyr molars are large. The buccolingual diameter of M^2 exceeds recent African and Eurasian UP sample means by more than 2 SD (table S3). Radiographs reveal cynodont molars,



Fig. 1. The Hofmeyr skull in facial (top row), right lateral (middle row), and superior (bottom row) views as it appeared in 1968 and 1998. Note the initial state of preservation of the skull, and the antemortem damage to the supraorbital torus and lateral margin of the right orbit.

although pulp chamber height is likely to have been affected by the deposition of secondary dentine in these heavily worn teeth.

Thus, Hofmeyr is seemingly primitive in comparison to recent African crania in a number of features, including a prominent glabella; moderately thick, continuous supraorbital tori; a tall, flat, and straight malar; a broad frontal process of the maxilla; and comparatively large molar crowns. Hofmeyr is contemporaneous with later Eurasian Neandertals, but it clearly does not evince the cranial and mandibular apomorphies that define that clade (28). This is not surprising, given its geographic location. Although Hofmeyr is similar in size to Eurasian UP crania, it differs from them in other respects (such as its broad nose and continuous supraorbital tori).

In order to assess the phenetic affinities of Hofmeyr to penecontemporaneous Eurasian UP and recent humans, we conducted multivariate morphometric analyses of 3D landmark coordinates and linear measurements of crania representing these populations. We digitized 19 3D coordinates of landmarks that represent as fully as possible the currently preserved anatomy of the Hofmeyr skull (table S4). These were compared with homologous data for recent human samples from five broad geographic areas (North Africa, sub-Saharan Africa, Western Eurasia, Oceania, and Eastern Asia/New World). The sub-Saharan sample was divided into Bantu-speaking (Mali and Kenya) and South African Khoe-San samples. The latter are represented in the Holocene archaeological record of the subcontinent, and inasmuch as they are the oldest historic indigenes of southern Africa, they might be expected to have the closest affinity to Hofmeyr (12). The North African sample consists of Epipaleolithic (Mesolithic) individuals that provide a temporal depth of approximately 10,000 years. The 3D data were also compared for two Neandertal, four Eurasian UP, and one Levantine early modern human fossils (table S5). The landmark coordinate configurations for each specimen were superimposed with the use of generalized Procrustes analysis and analyzed with a series of multivariate statistical techniques (29).

Hofmeyr falls at the upper ends of the recent sub-Saharan African sample ranges and within the upper parts of all other recent human sample ranges in terms of centroid size (fig. S6). In a canonical variates analysis of these landmarks (Fig. 2), axis 1 separates the sub-Saharan African samples from the others, and axis 4 tends to differentiate the UP specimens from recent homologs. Hofmeyr clusters with the UP sample, and although it falls within the recent human range on both axes, it is outside the 95% confidence ellipse for the Khoe-San sample and barely within the limits of the other sub-Saharan African sample. These canonical axes are weakly correlated with centroid size, which emphasizes that the similarity between Hofmeyr and the UP sample is due only in small part to similarity in size.

Fig. 2. Canonical variates analysis of recent and fossil samples showing 95% confidence ellipses for recent samples. Symbol abbreviations are as follows: HOF (Hofmeyr), EUP (Eurasian Upper Paleolithic), EMH (Skhul 5 early modern human), and NDT (Neandertals). Ellipses represent 95% confidence ellipses for recent human samples: SAN (South African Khoe-San), AFR (sub-Saharan Africa), WEU (Western Eurasia), OCE (Oceania), and EAS (East Asia/New World).

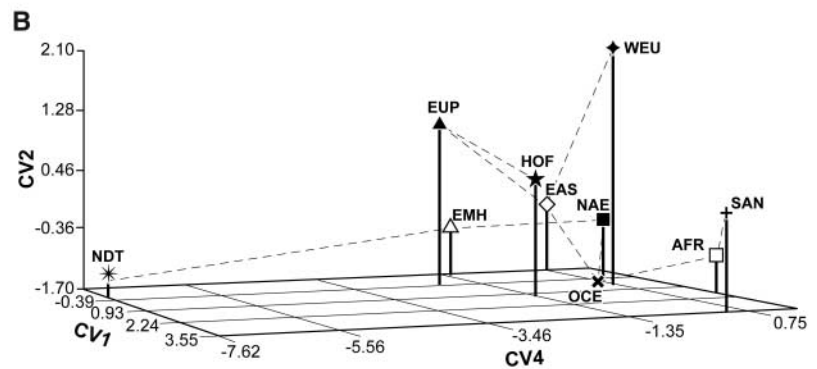
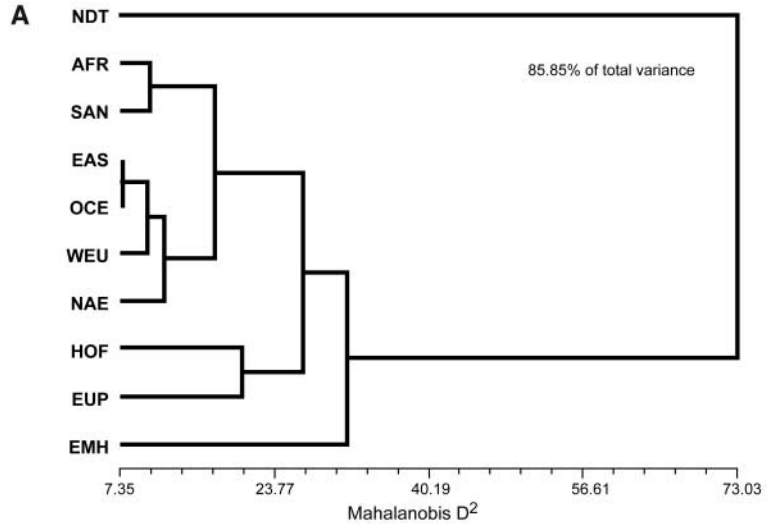
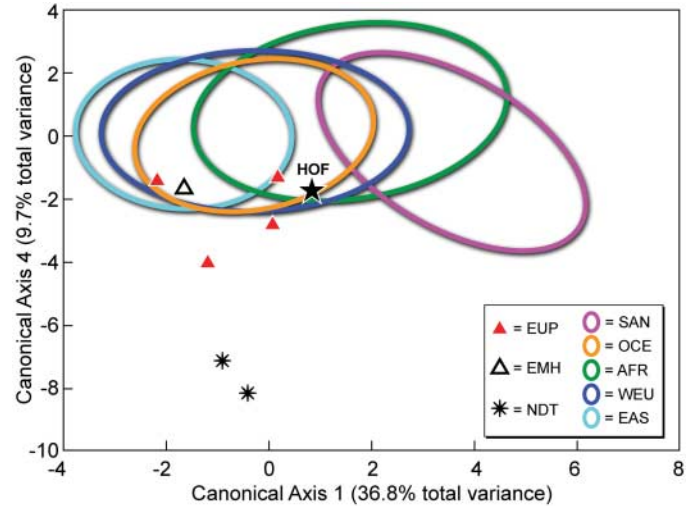


Fig. 3. Phenetic affinities of the Hofmeyr (HOF) cranium determined from 3D coordinates landmarks. (A) UPGMA tree based on Mahalanobis D^2 distances (corrected for unequal sample sizes) among samples. (B) Minimum spanning tree representing the closest links based on the total variance of all 21 principal components from which the canonical variates analysis was calculated. Sample abbreviations are as follows: AFR (sub-Saharan Africa), EAS (East Asia/New World), EMH (early modern human = Skhul), EUP (Eurasian Upper Paleolithic), NAE (North African Epipaleolithic), NDT (Neandertal), OCE (Oceania), SAN (South African Khoe-San), and WEU (Western Eurasia).

Mahalanobis squared distances among samples were calculated to establish the group to which Hofmeyr has the greatest similarity (table S6). Hofmeyr shows low posterior and typicality probabilities for all recent humans, but much higher probabilities for the UP sample (posterior 0.76, typicality 0.43). The unweighted pair group method with arithmetic average (UPGMA) cluster and 3D minimum spanning trees calculated from the Mahalanobis generalized (D^2) distances highlight Hofmeyr's phenetic affinity to the UP specimens and its distinction from recent sub-Saharan Africans (Fig. 3). The high success rate of cross-validation classification lends confidence to these results: ~80% of recent human crania are correctly classified to their geographic sample when this approach is used (29).

We sought to further assess the relationship between the Hofmeyr cranium and samples of various recent sub-Saharan Africans ($n = 263$) and Europeans ($n = 24$) and a small sample of UP Eurasians ($n = 5$), using eight linear dimensions of the face and cranial vault (table S7). The recent sub-Saharan African samples consisted of several Bantu-speaking groups that were combined because no significant differentiation among them was observed through analyses of variance.

The craniofacial variables were size-adjusted by transforming them into Z- and C-scores following Howells (11) and were analyzed by factor analysis with varimax rotation following Ribot (13). Analyses of variance of the regression factor scores indicate that factor 2 provided the greatest differentiation among the comparative samples. Therefore, this was used preferentially to identify the position of Hofmeyr vis-à-vis the 95% confidence ellipses of these samples. Hofmeyr is encompassed by the variation exhibited by Late Pleistocene Eurasian

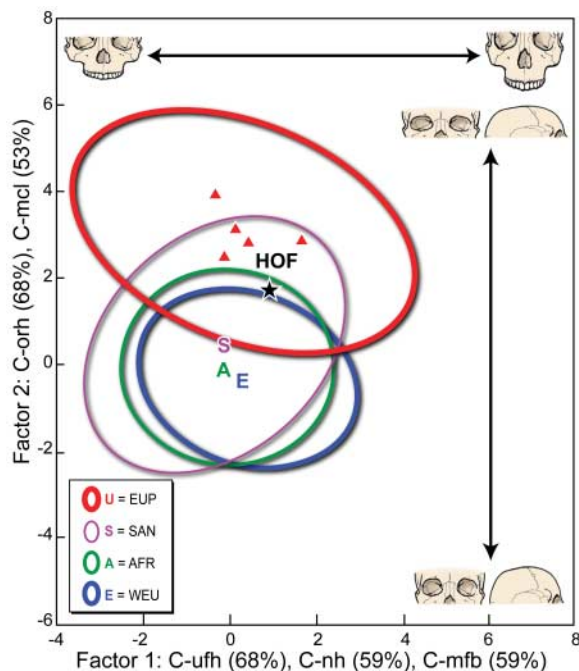
crania (Fig. 4). It is also encompassed by the 95% confidence ellipse of the recent Khoe-San and sub-Saharan Bantu-speaker samples, but falls just beyond the 95% confidence ellipse of recent Europeans. These observations are supported by the proximity matrix of squared Euclidean distances derived from the regression factor scores, which reveal the UP Eurasian sample as closest to Hofmeyr (table S8).

Hofmeyr and the UP Eurasian specimens tend to have comparatively high loadings on factor 2, which is indicative of a trend toward relatively longer crania with relatively shorter orbits than those in recent populations from these same geographic areas. This perhaps attests to a common trend for change in craniofacial shape over the past 36,000 years in both Eurasia and sub-Saharan Africa.

The results of the 3D geometric and linear morphometric analyses suggest that Hofmeyr shares close affinity with Eurasian UP specimens but is more distant from recent sub-Saharan African populations. These analyses emphasize that neither large absolute size nor allometrically related shape similarities are responsible for the relationship seen between Hofmeyr and penecontemporaneous Eurasian UP skulls.

The placement of Hofmeyr with Eurasian UP crania rather than with recent, geographically proximate humans is important given the specimen's geochronological age and the ability of craniometric data to differentiate recent human populations in accord with their geographic and genetic relationships. Our findings are consistent with the hypothesis that UP Eurasians descended from a population that emigrated from sub-Saharan Africa in the Late Pleistocene. The Hofmeyr cranium affords potential insights into the morphology of such a population.

Fig. 4. Plot of regression factor scores of linear measurements recorded for Hofmeyr (HOF, star), Eurasian UP crania (EUP, triangles), and recent Khoe-San (SAN), sub-Saharan African (AFR), and Western Eurasian (WEU) samples. The 95% confidence ellipses for the UP and recent samples and the centroids of the recent samples (letters S, A, and E) are shown. This analysis expresses 50% of the total variance in the first two factors (factor 1 = 29%, factor 2 = 21%). Factor 1 accounts for 68% of the variance of upper facial height (C-ufh), 59% of the variance of nasal height (C-nh), and 59% of the variance of minimum frontal breadth (C-mfb). Factor 2 accounts for 68% of the variance of orbital height (C-orh) and 53% of the variance of maximum cranial length (C-mcl). Crania to the right of the plot exhibit tall faces, and crania to the bottom of the plot exhibit long vaults and short orbits. The samples are described in (29).



References and Notes

1. M. Ingman, H. Kaessmann, S. Pääbo, U. Gyllenstein, *Nature* **408**, 708 (2000).
2. P. Forster, *Philos. Trans. R. Soc. London Ser. B* **359**, 255 (2004).
3. T. Kivisild et al., *Genetics* **172**, 373 (2006).
4. N. Ray, M. Currat, P. Berthier, L. Excoffier, *Genome Res.* **15**, 1161 (2005).
5. V. Macaulay et al., *Science* **308**, 1034 (2005).
6. T. Takasaka et al., *Am. J. Phys. Anthropol.* **129**, 465 (2006).
7. S. H. Ambrose, *J. Archaeol. Sci.* **25**, 377 (1998).
8. P. Mellars, *Nature* **439**, 931 (2006).
9. V. Eswaran, H. Harpending, A. R. Rogers, *J. Hum. Evol.* **49**, 1 (2005).
10. D. Garrigan, Z. Mobasher, T. Severson, J. A. Wilder, M. F. Hammer, *Mol. Biol. Evol.* **22**, 189 (2005).
11. W. W. Howells, *Skull Shapes and the Map. Craniometric Analyses in the Dispersion of Modern Homo* (Papers of the Peabody Museum, vol. 79, Harvard Univ. Press, Cambridge, MA, 1989).
12. M. M. Lahr, *The Evolution of Modern Human Diversity. A Study of Cranial Variation* (Cambridge Univ. Press, Cambridge, 1996).
13. I. Ribot, *Bull. Mem. Soc. Anthropol. Paris* **16**, 143 (2004).
14. C. C. Roseman, T. D. Weaver, *Am. J. Phys. Anthropol.* **125**, 257 (2004).
15. K. Harvati, T. D. Weaver, *Anat. Rec.* **288A**, 12251 (2006).
16. D. Turbon, A. Pérez-Pérez, C. B. Stringer, *J. Hum. Evol.* **32**, 449 (1997).
17. J. C. Vogel, *S. Afr. Archaeol. Bull.* **24**, 56 (1969).
18. J. Hawks, M. H. Wolpoff, *Quat. Int.* **75**, 41 (2001).
19. T. Higham, personal communication. The percentage of nitrogen in the whole bone was measured, because this is a reasonable correlate of remaining protein; the result of 0.06% N showed that the bone almost certainly contains insufficient collagen for AMS dating.
20. M. J. Aitken, *An Introduction to Optical Dating* (Oxford Univ. Press, Oxford, 1998).
21. K. R. Ludwig, *UIISO—A Program for Calculation of ^{230}Th - ^{234}U - ^{238}U Isochrones* (USGS Open File Report 93-531, U.S. Geological Survey, Reston, VA, 1993).
22. J. F. Briesmeister, *MCNP—A General Monte Carlo N-particle Transport Code Version. 4C* (report LA-13709-M, Los Alamos National Laboratory, Los Alamos, NM, 2000).
23. R. P. Nathan et al., *Rad. Meas.* **37**, 305 (2003).
24. Details on methods relating to geochronological age determination (in materials and methods, chronology) are available as supporting material on Science Online.
25. H. de Villiers, *The Skull of the South African Negro. A Biometrical and Morphological Study* (Witwatersrand Univ. Press, Johannesburg, South Africa, 1968).
26. F. H. Smith, J. F. Simek, M. S. Harrill, in *The Human Revolution: Behavioral and Biological Perspectives on the Origins of Modern Humans*, P. Mellars, C. B. Stringer, Eds. (Edinburgh Univ. Press, Edinburgh, 1989), pp. 172–193.
27. J. Szilvassy, H. Krietscher, E. Vlcek, *Ann. Vienna Nat. Hist. Mus.* **89**, 313 (1987).
28. E. Trinkaus, *Curr. Anthropol.* **47**, 597 (2006).
29. Details on methods relating to the 3D geometric and linear morphometric analyses (materials and methods, morphometric analyses) are available as supporting material on Science Online.
30. We thank the late W. W. Howells for sharing his craniometric data; L. Betti-Nash and M. Stewart for artwork and photography; and R. G. Roberts, F. James Rohlf, and anonymous reviewers for their helpful comments. This research was supported by grants from the Wenner-Gren Foundation, the Leakey Foundation, the American Philosophical Society, and the National Geographic Society to F.E.G. and the National Environment Research Council to R.M.B.

Supporting Online Material

www.sciencemag.org/cgi/content/full/315/5809/226/DC1
Materials and Methods
Figs. S1 to S6
Tables S1 to S8
References

13 October 2006; accepted 27 November 2006
10.1126/science.1136294